Characterization of AlN-based Ceramic Composites for Use as Millimeter Wave Susceptor Materials at High Temperature: High Temperature Thermal Properties of AlN:Mo with 0.25% to 4.0% Mo by Volume

Brad W. Hoff[1], Frederick W. Dynys[2], Steven C. Hayden[3], Rachael O. Grudt[3], Martin S. Hilario[1], Anthony E. Baros[1], Michele L. Ostraat[3]

[1]*Air Force Research Laboratory, Kirtland AFB, NM, 87117, USA*

[2]*NASA Glenn Research Center, Cleveland, Ohio 44135, USA*

[3]*Aramco Research Center – Boston, Aramco Services Company, Cambridge, MA 02139, USA*

ABSTRACT

In order to begin to evaluate and model the suitability of high temperature ceramic composites, such as AlN:Mo, as susceptor materials for power beaming applications, the electromagnetic, thermal, and mechanical properties of the material must be known at elevated temperatures. Work reported here focuses on the development of thermal property datasets for AlN:Mo composites ranging from 0.25% to 4.0% Mo by volume. To calculate thermal conductivity of the AlN:Mo composite series, specific heat capacity, thermal diffusivity, and density data were acquired. The calculated specific heat capacity, C_p, of the set of AlN:Mo composites was, on average, found to be approximately 803 J/kgK at 100 °C and to increase to approximately 1133 J/kgK at 1000 °C, with all values to be within +/- 32 J/kgK of the average at a given temperature. These calculated specific heat capacity values matched values derived from DSC measurements to within the expected error of the measurements. Measured thermal diffusivity, α, of the set of AlN:Mo composites was, on average, found to be approximately 3.93 x 10^{-1} cm^2/s at 100 °C and to increase to approximately 9.80 x 10^{-2} cm^2/s at 1000 °C, with all values within +/- 1.84 x 10^{-2} cm^2/s of the average at a given temperature. Thermal conductivity, k, for the set of AlN:Mo composites was found to be approximately 108 W/mK at 100 °C and to decrease to approximately 38 W/mK at 1000 °C, with all values within +/- 5.3 W/mK of the average at a given temperature.

Data trends show that increasing Mo content correlates to lower values of of C_p, α, and k at a given temperature.

1. INTRODUCTION:

In some wireless power transfer systems employing thermo-mechanical conversion methodologies [1]–[3], bulk susceptor materials are required to convert microwave or millimeter wave radiation into thermal power, which is, in turn, converted into electrical power by external means. These bulk susceptor materials may take the form of composite materials generated through the combination of a high-thermal-conductivity ceramic matrix and radiation-absorbing additives, such as lossy ceramics or metal particles [1].

For ease of design, the effective dielectric loss of the susceptor composite should be dominated by contributions from the additive material. Additionally, the temperature-dependent dielectric loss of the composite should be as weakly exponential as achievable, in order to limit the likelihood of thermal runaway effects [4] and to better enable optimal material performance over a wide range of operating temperatures.

One such ceramic composite system presently under investigation for use as a W-band (75 GHz – 110 GHz) mm-wave susceptor material is aluminum nitride containing metallic molybdenum powder (AlN:Mo). In order to evaluate and model [5] the suitability of such AlN:Mo composites as susceptor materials, the electromagnetic, thermal, and mechanical properties of the material must be known at elevated temperatures.

The work described herein focuses on the thermal properties of commercially available [6], hot pressed AlN:Mo composites in the additive range of 0.25% to 4% Mo (by volume). AlN:Mo composites with Mo loading in this range have been identified as likely candidate materials for future power beaming experiments by the coauthors [1]. As described in Ref. [5], multiphysics modeling of ceramic composites in a heat exchanger configuration requires temperature-dependent specific heat capacity (C_p) data (at constant pressure) and thermal conductivity (k) data over the temperature range of interest.

2. X-RAY DIFFRACTION (XRD) COMPOSITIONAL ANALYSIS

For crystallinity and phase analysis, x-ray diffraction (XRD) was performed using a Bruker D8 Discover diffractometer equipped with a copper tube ($l = 0.15418$ nm), and a VANTEC-500 2-D detector. XRD spectra were measured with a 2θ range of $10°$ to $100°$ in steps of $15°$, with a collection time of 300 s per step. XRD characterization data for weight percentage analysis were collected with 2θ range of $15°$ to $105°$ in steps of $10°$, again with a collection time of 300 s per step. XRD spectra and structural information for 4 phases (AlN, Mo, Mo_2C, and $YAlO_3$) were imported into Bruker DIFFRAC.TOPAS software, and Rietveld structural refinement was utilized to ascertain the weight percentage of each phase.

The XRD analysis (Figure 1) revealed a highly crystalline AlN matrix with non-matrix phase concentrations that increased with nominal loading percentages, as is evidenced by the increasing intensity of the Mo peaks across the series (Figure 1, zoom). Peaks associated with the Mo_2C phase appear at 0.5% loading and remain approximately the same in intensity with further loading, and $YAlO_3$ peaks have constant intensity across all Mo loadings. Phase breakdowns attained via Rietveld refinement of the XRD data are provided in Figure 2, where AlN is the balance. The $YAlO_3$ phase forms during the sintering process as a product of the reaction between Al_2O_3 (present on the surface

layers of un-sintered matrix AlN particles) and the sintering aid additive (Y_2O_3) [7]–[9]. It is also noted that added Mo was found to react with carbon present in the matrix [7], [10] to form Mo_2C up to an estimated concentration threshold of approximately 0.5% by volume. Beyond this threshold, additional Mo remains in the metallic state (Figure 2).
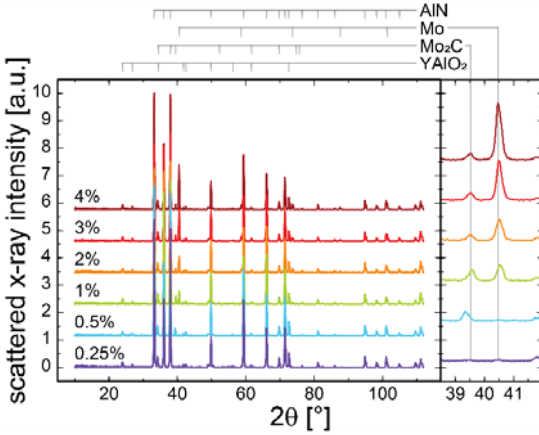

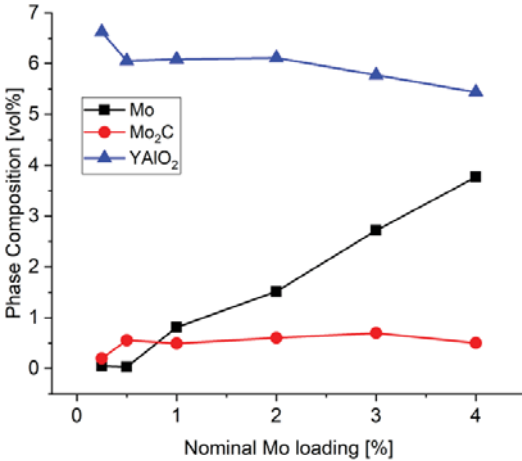Figure 1. X-ray diffraction patterns AlN:Mo ceramic composites ranging from 0.25% to 4.0% Mo by volume.

Figure 2. Phase analysis providing estimated volume percentages for AlN composites loaded with Mo at the nominal loading percentages as indicated.

3. DENSITY AND THERMAL PROPERTY CHARACTERIZATION

3.1 Density Measurements

AlN:Mo sample density was measured by the Archimedes method using methyl ethyl ketone as the fluid. Measured densities are plotted in Figure 3 as a function of Mo content. AlN:Mo composite density, ρ, exhibits a linear relationship with percent Mo content (by volume), as described by Equation (1).

$$\rho = \left((\%Mo \ by \ vol.) * 6.77 \times 10^{-2} + 3.30\right) \ g/cm^3 \quad (1)$$
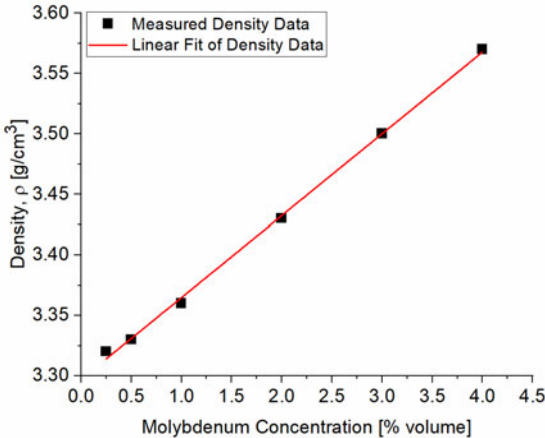
Figure 3. Measured density of AlN:Mo ceramic composites ranging from 0.25% to 4.0% Mo by volume.

3.2 Specific Heat Capacity Calculations, Measurements, and Results

Values for specific heat capacity at constant pressure (C_p) for all six AlN:Mo compositions were calculated for temperatures up to 1000 °C. The specific heat capacity was calculated utilizing the rule of mixtures for AlN, Mo, Mo_2C, and $YAlO_3$ under the assumption of non-reactivity between the phases [11]–[13]. Specific heat capacity data for constituent materials from NIST [14] (AlN and Mo); Liu, et al. [15] (Mo_2C); and Hurst, et al. [16] ($YAlO_3$, using Kopp's Law) were used to calculate the composite specific heat capacity. Plots of calculated specific heat capacity data are displayed in Figure 4.

Three of the six AlN:Mo compositions (0.25%, 0.5%, and 1.0% Mo by vol.) were measured using differential scanning calorimetry (DSC). Sample masses for the 0.25%, 0.5%, and 1.0% Mo (by vol.) compositions used for DSC analysis were 56.8 mg, 59.5 mg, and 59.3 mg, respectively. The DSC utilized for the measurements was a TA Instruments SDT Q600. Platinum crucibles, having a thin layer of yttria on the bottom, contained the samples during measurement. A sapphire sample was used as the standard for the measurements. A heating rate of 20 °C/min was implemented for measurements of baselines, the sapphire standard, and the samples. Argon gas, at a flow rate of 50 mL/min, was used as the purge gas during measurements.

Specific heat capacity (C_p) values for the three AlN:Mo compositions were derived from DSC heat flux measurement data in the manner described by Ref. [17]. The measured C_p data are compared to calculated C_p data for AlN/Mo composites, as shown in Figure 4 for temperatures up to 600 °C. Uncertainty of C_p values obtained using DSC is +/- 5% from 30 °C to 600 °C. The data trend shows that increasing Mo content corresponds to reduced C_p values. The measured data exhibit a larger reduction of C_p with increasing Mo content than do the calculated data.
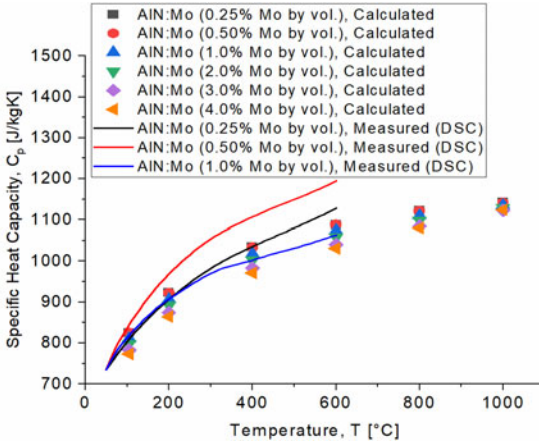

Figure 4. High temperature calculated and measured specific heat capacity data for AlN:Mo composites ranging from 0.25% to 4.0% Mo by volume.

3.3 Thermal Diffusivity Measurements and Results

The laser flash method [18], [19] was used to measure thermal diffusivity (α) of disc-shaped samples with nominal dimensions of 2-3 mm thickness and 12.5 mm diameter. Laser flash diffusivity measurements were performed using a Flashline 5000 (Anter Corporation, Pittsburg, PA), and thermal diffusivity data was analyzed using the Clark and Taylor method [20]. Samples were measured in accordance with ASTM E1461 [21]. Specimens were coated with carbon on both sides to ensure a consistent emissivity and absorption. Thermal diffusivity was measured in the temperature range of 100 to 1000 °C in a N_2 atmosphere.

The measured thermal diffusivity data are presented in Figure 5. Each plotted value is an average of three measurements. Measured thermal diffusivity data are compared to previously published data for hot pressed AlN and AlN:Mo (30% Mo by vol.) from Khan et al. [11]. Measured thermal diffusivity values for the authors' AlN:Mo composites were found to be slightly higher than those of Khan et al. at temperatures up to 600 °C. Above 600 °C, the 30% Mo composite of Khan et al. was found to have thermal diffusivity values approximately equal to the average of the measured thermal diffusivity values for the authors' composites for a given temperature.
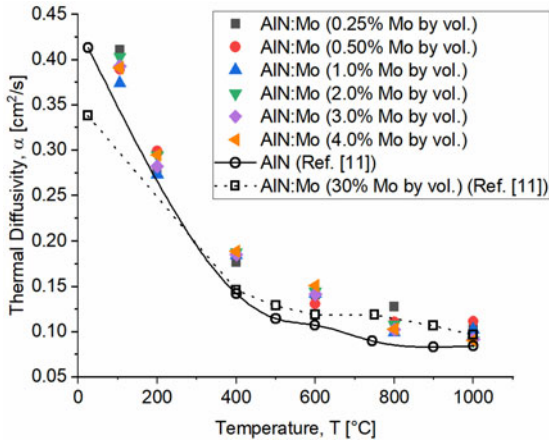
Figure 5. High temperature thermal diffusivity data for AlN:Mo composites ranging from 0.25% to 4.0% Mo by volume. Measured data is overlaid with literature data for hot-pressed AlN and AlN:Mo (30% Mo by vol.) from Khan et al. [11].

3.4 Thermal Conductivity Calculations, Results, and Discussion

The thermal conductivity (k) of AlN is dependent on processing additives, such as yttrium and lanthanide compounds, used to assist densification and oxygen removal during sintering [9]. The presence of free oxygen during densification enables aluminate phase formation, which has a direct negative effect on thermal conductivity. Typically, thermal conductivity of AlN realizes a maximum between 5-8% (vol.) sintering additive [9].

Thermal conductivity (k) can be calculated from thermal diffusivity (α), density (ρ) and specific heat capacity (C_p): $k = \alpha\rho C_p$. The uncertainty in k is estimated to be 10%. Figure 6 shows temperature dependent thermal conductivity data for AlN:Mo composites (k_c) with Mo concentrations of 0.25% to 4.0% by vol. The results show no strong dependence on Mo content. Literature data for elemental Mo [22] and hot pressed AlN with Y_2O_3 additives [9] are also plotted in Figure 6 for reference. The k_c temperature dependence is dominated by the AlN matrix, showing a strong reduction in thermal conductivity with increasing temperature. The k_c measurements generally fall below the literature values of the AlN (with 4% yttria by wt.) [9].
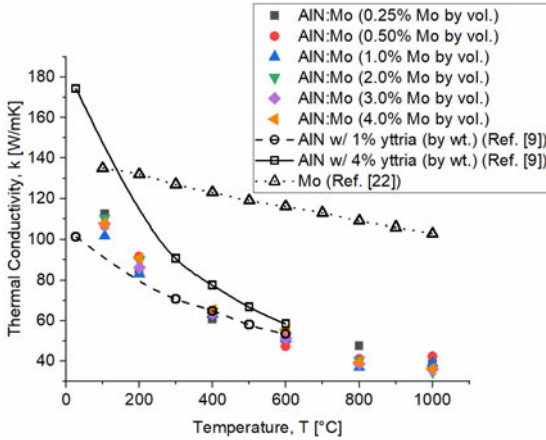
Figure 6. High temperature thermal conductivity data for AlN:Mo composites ranging from 0.25% to 4.0% Mo by volume. Experimental data is overlaid with literature data for AlN with 1% and 4 % yttria (by wt.) [9] and for Mo [22].

4. ANALYSIS

The thermal conductivity of a composite depends on constituent thermal conductivity, constituent volume fraction, minor constituent particle size and distribution, and the existence of an interfacial thermal barrier between the matrix and particle. Modeling by Hasselman and Johnson [23] shows the effective thermal conductivity of a continuous matrix with dilute volume fractions of non-interacting spherical inclusions as Equation (2).

$$k_c = k_m \left[2\left(\frac{k_d}{k_m} - \frac{k_d}{rh_c} - 1\right)V_d + \frac{k_d}{k_m} + \frac{2k_d}{rh_c} + 2 \right] / \left[\left(1 - \frac{k_d}{k_m} + \frac{k_d}{rh_c}\right)V_d + \frac{k_d}{k_m} + \frac{2k_d}{rh_c} + 2\right]$$

(2)

where k is the thermal conductivity; V_d is the volume fraction of the dispersed phase; subscripts c, m, and d refer to the composite, matrix, and dispersed phase, respectively; r is the radius of the particle inclusion; and h is the thermal boundary conductance. Equation (2) reduces to the Maxwell equation (Equation (3)) [24] for the case of no thermal interfacial resistance ($h_c = \infty$):

$$k_{c,(h_c=\infty)} = k_m \left[2\left(\frac{k_d}{k_m} - 1\right)V_d + \frac{k_d}{k_m} + 2 \right] / \left[\left(1 - \frac{k_d}{k_m}\right)V_d + \frac{k_d}{k_m} + 2\right]$$

(3)

In the opposite extreme, where h_c is assumed to be zero, Equation (2) reduces to Equation (4):

$$k_{c,(h_c=0)} = 2k_m \frac{(1-V_d)}{(2+V_d)}$$

(4)

The matrix thermal conductivity (k_m) for the particular AlN formulation used in the present study was stated by the vendor [6] to be 150 +/- 5 W/mK at 25 °C. The thermal conductivity of the molybdenum dispersed phase, k_d, at 25 °C was estimated to

be 137 W/mK using a linear regression of data from Ho et al. [22], as shown in Figure 7. Using the 4.0% Mo (vol.) AlN:Mo composite as a test case, the composite thermal conductivity (k_c) can be calculated using an exponential fit of the relevant experimental data (plotted previously in Figure 6), as depicted in Figure 7. Using this fit, k_c for the 4.0% Mo composite is estimated to be 127 W/mK at 25 °C. It becomes apparent that when the vendor-provided matrix thermal conductivity ($k_m = 150$ +/- 5 W/mK) and the dispersed phase thermal conductivity ($k_d = 137$ W/mK) are in excess of the measured thermal conductivity of the composite ($k_c = 124$ W/mK), the Maxwell equation (Equation (3)) overestimates the thermal conductivity of the present AlN:Mo material system as 149 W/mK (for $k_m = 150$).
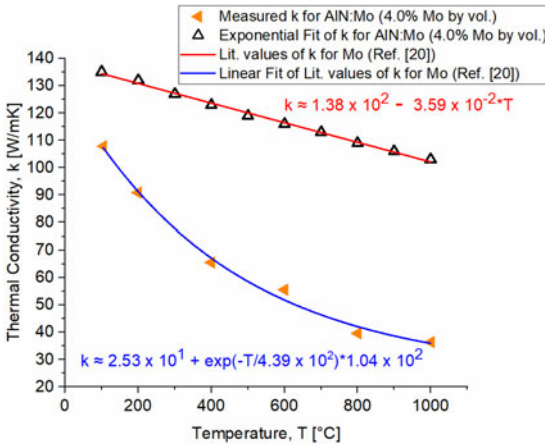

Figure 7. Measured thermal conductivity data for AlN:Mo (4.0% Mo by vol.), literature values of thermal conductivity for Mo from Ref. [22], and associated curve fits.

The method of Hasselman and Johnson [23] (Equation (2)) can be used to determine if the drop in thermal conductivity of the composite, compared to the matrix, can be readily explained by the presence of finite thermal interfacial resistance (h_c) at the boundary of the dispersed Mo particles. For the purposes of this determination, the authors note that: 1) uncertainty in the thermal conductivity of the present AlN:Mo composite is taken into account, 2) the range of vendor-provided matrix thermal conductivity values is taken into account without accounting for additional uncertainty, 3) dispersed phase thermal conductivity and volume fraction of the dispersed phase will be treated as exact (i.e., uncertainty is ignored), and 4) assumptions implicit in the Hasselman and Johnson model, such as the requirement that the material system be far from the percolation threshold, remain in effect. The relevant values for this determination are: experimentally determined k_c (AlN:Mo, 4% Mo by vol.) = 124 W/mK +/- 10%, $k_m = 150$ +/- 5 W/mK, $k_d = 137$ W/mK, $V_d = 0.04$.

Using calculations based on Equation (2), curves of k_c for three k_m values (145 W/mK, 150 W/mK, and 155 W/mK), are plotted in Figure 8 for a wide range of values of rh_c. This term represents the radius of the particle inclusions (r) multiplied by the thermal interfacial resistance (h_c). The upper and lower asymptotes of the k_c curves represent values calculated by Equation (3) and Equation (4), respectively.

Experimental values for the AlN:Mo (4% Mo by vol.) composite k_c are overlaid with the Equation (2) k_c curves. The calculated and experimental curve sets approach at the lowest values of rh_c for the 4% Mo composite (the shaded region in Figure 8) but do not overlap; thus, a finite h_c at the Mo particle boundaries does not adequately account for the reduction in thermal conductivity observed in the composite (compared to the virgin AlN matrix). Because the independent variable was chosen as rh_c and due to the asymptotic response of the function at extreme values, any combination of particle radius and thermal barrier resistance that satisfies the assumptions of Hasselman and Johnson's effective medium model will represent a composite having a thermal conductivity value that falls somewhere between the upper and lower asymptotes of the curve representing the assumed k_m value.
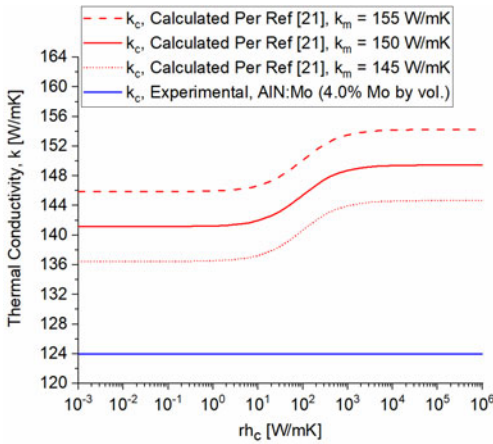

Figure 8. Calculated k_c value curves, based on Equation (2) [23], overlaid with experimental k_c values for AlN:Mo (4.0% Mo by vol.)

As described previously, the thermal conductivity of AlN is extremely sensitive to the presence of free oxygen during the sintering process [7]–[9]. The authors believe that a significant contributor to the reduction in thermal conductivity of the AlN:Mo composite, compared to the virgin AlN matrix, is due to the inadvertent addition of oxygen when Mo is added to the matrix material prior to sintering. Chhillar et al. indicate that due to the relatively large surface area of the Mo microparticles, formation of thin oxide layers or layers of adsorbed free oxygen are possible [25]. Thus, pretreatment of the Mo powder to remove oxygen [26] or the adjustment of oxygen-gettering sintering additive concentrations [7], [9] may potentially enable AlN:Mo composites with higher thermal conductivity.

4. SUMMARY

In order to begin to evaluate and model the suitability of high temperature ceramic composites, such as AlN:Mo, as susceptor materials for power beaming applications, the electromagnetic, thermal, and mechanical properties of the material must be known at elevated temperatures. Work reported here focused on the

development of thermal property datasets for AlN:Mo composites ranging from 0.25% to 4.0% Mo by volume.

To calculate thermal conductivity of the AlN:Mo composite series, specific heat capacity, thermal diffusivity, and density data were acquired. The calculated specific heat capacity, C_p, of the set of AlN:Mo composites was, on average, found to be approximately 803 J/kgK at 100 °C and to increase to approximately 1133 J/kgK at 1000 °C, with all values found to be within +/- 32 J/kgK of the average at a given temperature. These calculated specific heat capacity values matched values derived from DSC measurements to within the expected error of the measurements. Measured thermal diffusivity, α, of the set of AlN:Mo composites was, on average, found to be approximately 3.93 x 10^{-1} cm^2/s at 100 °C and to increase to approximately 9.80 x 10^{-2} cm^2/s at 1000 °C, with all values within +/- 1.84 x 10^{-2} cm^2/s of the average at a given temperature. The measured density, ρ, of the set of AlN:Mo composites was found to vary linearly with added Mo and to follow the relationship described by Equation (1). Thermal conductivity, k, for the set of AlN:Mo composites was found to be approximately 108 W/mK at 100 °C and to decrease to approximately 38 W/mK at 1000 °C, with all values within +/- 5.3 W/mK of the average at a given temperature. Data trends show increasing Mo content correlates to reductions of C_p, α, and k at a given temperature.

Comparisons of composite thermal conductivity predicted using the method of Hasselman and Johnson [23] (Equation (2)) and experimentally measured values of the present AlN:Mo composites suggest that the process of adding Mo to the virgin AlN matrix material results in an overall reduction of thermal conductivity that cannot be explained by the thermal conductivity of the Mo grains even if finite thermal interfacial resistance at the grain boundaries is taken into account. The inadvertent addition of oxygen when the Mo is added to the matrix material prior to sintering may be a significant contributor to the reduction in thermal conductivity of the AlN:Mo composite (compared to the virgin AlN matrix). As a result, that pretreatment of the Mo powder to remove oxygen or adjustment of oxygen-gettering sintering additive concentrations may enable AlN:Mo composites with higher thermal conductivity.

ACKNOWLEDGMENTS

REFERENCES

1. B.W. Hoff, M.S. Hilario, B. Jawdat, A.E. Baros, F.W. Dynys, J.A. Mackey, V. V. Yakovlev, C.E. Andraka, K.M. Armijo, E. Savrun, and I.M. Rittersdorf, in 2018 Proc. IMPI's 52nd Annu. Microw. Power Symp. (International Microwave Power Institute, Long Beach, CA, 2018), pp. 82–83.

2. B.W. Hoff, M. Hilario, B. Jawdat, D. Agrawal, M. Lanagan, J. Cheng, and F. Dynys, in Proc. 12th Pacific Rim Conf. Ceram. Glas. Technol. (The Americal Ceramic Society, Waikoloa, HI, 2017), p. 61.

3. M.S. Hilario, B.W. Hoff, M.P. Young, and M.T. Lanagan, in 53rd AIAA Aerosp. Sci. Meet. (AIAA SciTech Forum, Kissimmee, FL, 2015), pp. 1–10.

4. J.M. Gaone, B.S. Tilley, and V. V. Yakovlev, in 2017 IEEE MTT-S Int. Microw. Symp. (IEEE, 2017), pp. 459–462.

5. V. V. Yakovlev, S.M. Allan, M.L. Fall, and H.S. Shulman, in Microw. RF Power Appl., edited by J. Tao (Cépaduès Éditions, Toulouse, 2011), pp. 303–306.
6. "Sienna Technologies, Inc." [Online]. Available: http://siennatech.com/. [Accessed: 06-Nov-2018].

7. J.H. Cooper, Process-Dependence of Properties in High Thermal Conductivity Aluminum Nitride Substrates for Electronic Packaging, Naval Postgraduate School, 1991.

8. G.W. Prohaska and G.R. Miller, MRS Proc. **167**, 215 (1989).

9. T.B. Jackson, A. V. Virkar, K.L. More, R.B. Dinwiddie, and R.A. Cutler, J. Am. Ceram. Soc. **80**, 1421 (2005).

10. Y. Kurokawa, K. Utsumi, and H. Takamizawa, J. Am. Ceram. Soc. **71**, 588 (1988).

11. A.A. Khan and J.C. Labbe, J. Eur. Ceram. Soc. **17**, 1885 (1997).

12. A.A. Khan and J.C. Labbe, Mater. Sci. Eng. **A 230**, 33 (1997).

13. A.A. Khan and J.C. Labbe, J. Eur. Ceram. Soc. **16**, 739 (1996).

14. M.W. Chase, J. Phys. Chem. Ref. Data, Monogr. **9**, 1 (1998).

15. Y. Liu, Y. Jiang, R. Zhou, X. Liu, and J. Feng, Ceram. Int. **41**, 5239 (2015).

16. J.E. Hurst and B.K. Harrison, Chem. Eng. Commun. **112**, 21 (1992).

17. P. Gabbott, in edited by P. Gabbott (Blackwell Publishing Ltd., Oxford, UK, (2008), pp. 1–50.

18. W.J. Parker, R.J. Jenkins, C.P. Butler, and G.L. Abbott, J. Appl. Phys. **32**, 1679 (1961).

19. L. Vozár and W. Hohenauer, High Temp. - High Press. 35–36, 253 (2003).

20. L.M. Clark and R.E. Taylor, J. Appl. Phys. **46**, 714 (1975).

21. ASTM International, ASTM E1461−13 Standard Test Method for Thermal Diffusivity by the Flash Method (West Conshohocken, PA, 2016).

22. C.Y. Ho, R.W. Powell, and P.E. Liley, Thermal Conductivity of Selected Materials Part 2 (National Standard Reference Data Series 16, National Bureau of Standards, Washington, D.C., 1968).

23. D.P.H. Hasselman and L.F. Johnson, J. Compos. Mater. **21**, 508 (1987).

24. J.C. Maxwell, A Treatise on Electricity and Magnetism, Vol. I, 3rd ed. (Oxford University Press, Oxford, UK, 1904).

25. P. Chhillar, D. Agrawal, and J.H. Adair, Powder Metall. **51**, 182 (2008).

26. B.-S. Kim, E. Kim, H.-S. Jeon, H.-I. Lee, and J.-C. Lee, Mater. Trans. **49**, 2147 (2008).